EUROPEAN ORGANIZATION FOR NUCLEAR RESEARCH

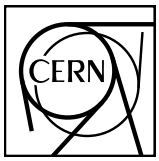

CERN-PH-EP-2014-089
09 May 2014

Beauty production in pp collisions at $\sqrt{s} = 2.76$ TeV measured via semi-electronic decays

The ALICE Collaboration*

Abstract

The production cross section of electrons from semi-leptonic decays of beauty hadrons in pp collisions at $\sqrt{s} = 2.76$ TeV at mid-rapidity ($|y| < 0.8$) in the transverse momentum range of 1-10 GeV/c with the ALICE experiment at the CERN LHC is reported. Electrons, other than those from the semi-electronic decays of beauty hadrons, were suppressed based on the impact parameter of the corresponding tracks. The production cross section of beauty decay electrons is compared to the result obtained with an alternative method which uses the difference in azimuth of heavy-flavour decay electrons and charged hadrons. Various perturbative QCD calculations are in agreement with the measured cross section within the experimental and theoretical uncertainties. The integrated visible cross section, $\sigma_{b\to e} = 3.47 \pm 0.40(\text{stat})^{+1.12}_{-1.33}(\text{sys}) \pm 0.07(\text{norm})$ μb, was extrapolated to full phase space using FONLL and the total $b\bar{b}$ production cross section, $\sigma_{b\bar{b}} = 130 \pm 15.1(\text{stat})^{+42.1}_{-49.8}(\text{sys})^{+3.4}_{-3.1}(\text{extr}) \pm 2.5(\text{norm}) \pm 4.4(\text{BR})$ μb, was obtained.

*See Appendix A for the list of collaboration members

1 Introduction

Perturbative Quantum Chromodynamic (pQCD) calculations [1, 2, 3] predict that heavy quarks (charm and beauty) are predominantly produced through the initial hard parton scattering processes. They are therefore of particular interest in pp collisions, as the measurement of their production provides essential tests of pQCD. Additionally, these results in pp collisions provide the necessary baseline for the corresponding measurements performed in heavy-ion collisions, which produce a high energy density QCD matter. Properties of this strongly interacting, deconfined partonic medium are studied using various heavy-quark observables [4, 5].

In pp collisions at $\sqrt{s}$ = 2.76 TeV, we have measured heavy-flavour hadron production utilizing the following: D mesons via hadronic decays (mid-rapidity) [6], heavy-flavour hadrons via semi-leptonic decays to electrons (mid-rapidity) and muons (forward rapidity) [7, 8], and J/ψ using di-muon (forward rapidity) and di-electron (mid-rapidity) decay channels [9]. Each measurement is in good agreement with pQCD (for inclusive $q\bar{q}$ production) or QCD-inspired models (for J/ψ). As both charm and beauty hadrons decay semi-leptonically the measured heavy-flavour decay muons and electrons have contributions from both. The objective of the analyses presented here is to obtain the total beauty production cross section by directly measuring the contribution of electrons from beauty hadron decays to the heavy-flavour decay electron transverse momentum (p_{T}) spectrum.

This paper presents the production cross section of electrons from semi-electronic decay of beauty hadrons measured in the mid-rapidity region ($|y| < 0.8$) with the ALICE detector for $1 < p_{\mathrm{T}} < 10$ GeV/c in pp collisions at $\sqrt{s}$ = 2.76 TeV. The total b$\bar{\mathrm{b}}$ production cross section based on the extrapolation to full phase space from the measured p_{T}-differential cross section is also presented. The results are compared to the predictions from three sets of pQCD calculations (FONLL [1], GM-VFNS [10], and k_{T}-factorization [3]). The results were obtained primarily using a track impact parameter analysis which takes advantage of the relatively long lifetime of beauty hadrons ($c\tau \sim 500$ μm) compared to charm hadrons. Along with the impact parameter method, an alternative method is presented which uses the difference in azimuth of heavy-flavour decay electrons and charged hadrons, $\Delta\varphi$. For beauty hadron decays the width of the near-side peak, $\Delta\varphi$ around zero, is indeed larger than that of charm hadron decays due to the decay kinematics of the heavier mass beauty hadrons. The difference can be exploited to extract the relative beauty contribution to the heavy-flavour decay electron sample, which can be used along with the measured heavy-flavour electron spectrum to compute the production cross section of electrons from beauty hadron decays.

2 Event and track selection

The data set from pp collisions at $\sqrt{s}$ = 2.76 TeV used for these analyses was recorded during the 2011 LHC run with ALICE [11, 12]. The impact parameter analysis was performed solely on a Minimum Bias (MB) sample while the electron-hadron correlation analysis was done using both the MB and Electromagnetic Calorimeter (EMCal) trigger samples. The MB collisions were triggered using the V0 detectors, located in the forward ($2.8 < \eta < 5.1$) and backward ($-3.7 < \eta < -1.7$) regions, and the Silicon Pixel Detector (SPD), which is the innermost part of the Inner Tracking System (ITS). The SPD consists of two cylindrical layers of hybrid silicon pixel assemblies, covering a pseudorapidity interval $|\eta| < 2.0$ and $|\eta| < 1.4$ for the inner and outer layer, respectively. The MB trigger required at least one hit in either of the V0 scintillator hodoscopes or in the SPD, in coincidence with the presence of LHC bunch crossings. Additional details can be found in [6]. The MB trigger cross section was measured to be 55.4$\pm$1.0 mb using a van der Meer scan [13]. In order to collect a larger data sample, MB events were triggered independently of the read-out state of the Silicon Drift Detector (SDD), which equips the two intermediate layers of the ITS. This resulted in a fraction of events lacking the SDD information. To have a homogeneously reconstructed sample of tracks, the SDD points were always excluded from the

track reconstruction used for these analyses. The EMCal Single Shower (SSh) trigger system generates a fast energy sum (800 ns) at Trigger Level 0 for overlapping groups of 4×4 ($\eta \times \varphi$) adjacent EMCal towers, followed by comparison to a threshold energy [14]. The data set recorded with the EMCal trigger demanded that the MB trigger condition was satisfied, and that at least one SSh sum exceeded a nominal threshold energy of 3.0 GeV. Additionally, events which satisfied the MB and EMCal trigger conditions were required to have a collision vertex with at least two tracks pointing to it and the vertex position along the beam line to be within ±10 cm of the nominal center of the ALICE detector. The results presented are based on 51.5 million MB events (integrated luminosity of 0.9 nb^{-1}) and 0.64 million EMCal trigger events (integrated luminosity of 14.9 nb^{-1}).

For both analyses the charged particle tracks were reconstructed in the Time Projection Chamber (TPC) [15] and ITS [16]. In the case of the EMCal based analysis these charged tracks were propagated to the EMCal and matched to clusters in the EMCal detector. The matching required the difference between the cluster position and extrapolated track point to be smaller than 0.025 units in η and 0.05 radians in φ. For both analyses, the requirement of hits in the SPD was employed to remove electrons that originated from photon conversions in the inner tracking detector material. For the impact parameter analysis the requirement on the displacement of the electron candidate from the collision vertex will be discussed in more detail in the following section.

Electrons were identified using the TPC, Time of Flight (TOF), and EMCal detectors [7]. For each analysis background hadrons, in particular charged pions, were rejected using the specific energy loss, dE/dx, measured for charged particles in the TPC. Tracks were required to have a dE/dx value between one standard deviation below and three standard deviations above the expected value for electrons. In the low momentum region (below 2.0 GeV/c for the impact parameter analysis and below 2.5 GeV/c for the correlation analysis) the candidates were required to be consistent within three standard deviations with the electron time of flight hypothesis. For higher transverse momentum, the TOF was not required, as the inclusion of a TOF cluster significantly reduced the electron selection efficiency. Additionally, the EMCal based correlation analysis used the energy deposited in the EMCal and E/p was required to be within 0.8 and 1.2 for electron candidates.

3 Analysis

3.1 Impact parameter technique

An inclusive electron measurement contains contributions from beauty and charm hadron decays along with background sources. The background is primarily composed of electrons from photon conversions in the beam-pipe and ITS material, π^0 and η Dalitz decays, and di-electron decays of light neutral vector mesons. In the inclusive sample, electrons from beauty decays can be enhanced by selecting on the displacement of the beauty hadron decay vertex from the primary vertex of the pp collision, as described in detail in [17].

The relatively long lifetime of beauty hadrons was exploited by selecting on the transverse impact parameter (d_0), which is the projection of the distance of closest approach vector of the charged track on the transverse plane, perpendicular to the beamline. The sign of d_0 is assigned according to the relative position of primary vertex and the track prolongation in the direction perpendicular to the direction of the p_{T} vector of the track. With the ALICE ITS the resolution on d_0 for this dataset, is less than 85 μm for $p_{\mathrm{T}} > 1$ GeV/c. Fig. 1 (a) shows the impact parameter distributions for all main contributions to the inclusive electron sample in the range $1 < p_{\mathrm{T}} < 6$ GeV/c. The distributions were obtained using a Monte Carlo (MC) simulation with GEANT3 [18], where the pp collisions were produced using the PYTHIA 6 event generator (Perugia-0 tune) [19]. Each source is characterized by a distinct d_0 distribution. Relative to that of beauty hadron decays, the d_0 distribution of electrons from Dalitz decays is relatively narrow, as they are produced at the collision vertex. The charm hadron decay and conversion

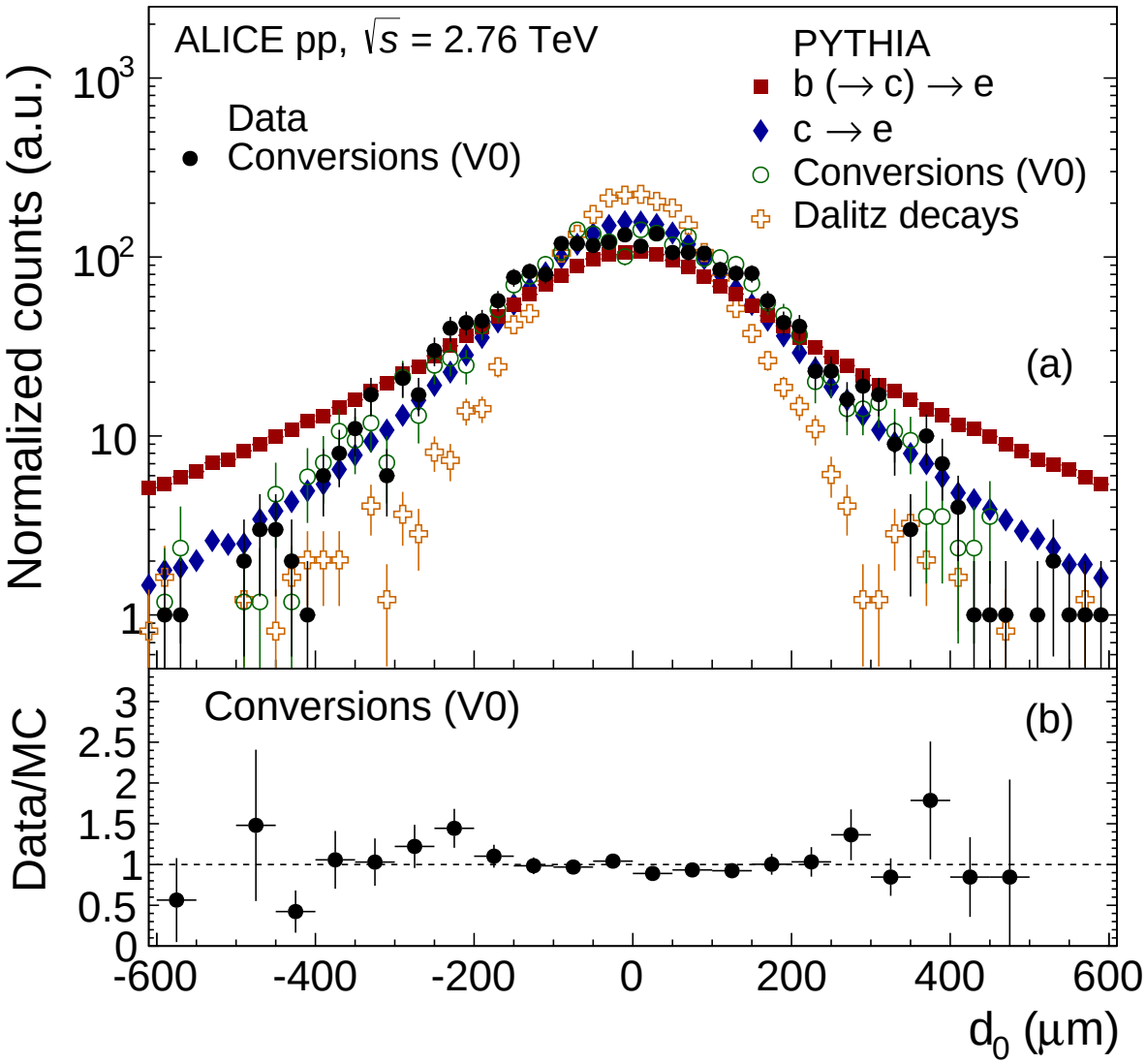

Fig. 1: (Color online) (a) Transverse impact parameter (d_0) distributions of electrons from beauty and charm hadron decays, decays of light hadrons, and photon conversions obtained from PYTHIA 6 simulations in the electron $p_{\rm T}$ range $1 < p_{\rm T} < 6$ GeV/c, along with the measured distribution of conversion electrons. The distributions are normalized to the same integrated yield. (b) Ratios of the measured and simulated d_0 distributions of conversion electrons in the ranges $1 < p_{\rm T} < 6$ GeV/c.

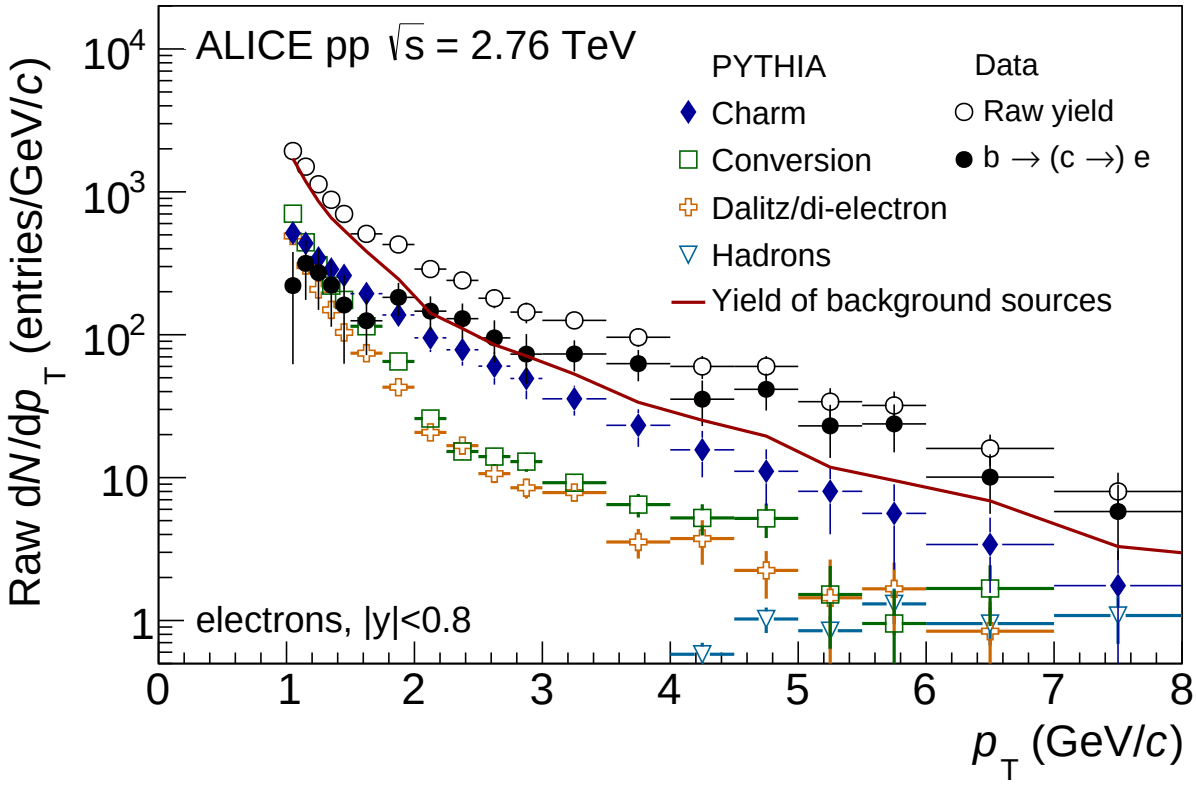

Fig. 2: (Color online) Raw spectrum of electrons from the impact parameter analysis (open circles) compared to background sources (from charm hadron decays, photon conversions, Dalitz decays, and hadron contamination) as a function of p_{T}. The background sources were obtained using a MC simulation. The raw yield after background sources are subtracted is also shown (closed circles).

electron d_0 distributions are broader than that of the Dalitz decay distribution as they emerge from secondary vertices, but are not as broad as those from beauty decays. For comparison, the d_0 distribution of conversion electrons from data is also shown in the figure. This pure sample of electrons from photon conversions in the detector material was identified using a V0-finder and an optimized set of topological selection requirements. Fig. 1 (b) shows the ratio of the impact parameter distribution from data to that from simulation in the range $1 < p_{\mathrm{T}} < 6$ GeV/c of the photon conversion electrons. The resulting ratio confirms a good agreement of the simulation and the selected electron candidates.

A selection on the d_0 parameter was applied in order to maximize the signal to background (S/B) ratio of electrons from beauty hadron decays. The requirement on the minimum impact parameter is p_{T} dependent as the width of the d_0 distribution depends on p_{T}. The S/B ratio varies due to the different impact parameter selection efficiencies for the various sources in various p_{T} regions. Therefore, separate p_{T} dependent parameterizations of the d_0 selection requirement were obtained for the analyses which utilize TPC-TOF and TPC only for electron selection. Electrons which satisfied the condition $|d_0| > 64 + 480 \cdot \exp(-0.56\ p_{\mathrm{T}})$ (with d_0 in μm and p_{T} in GeV/c) were used in the TPC-TOF analysis, while $|d_0| > 54 + 780 \cdot \exp(-0.56\ p_{\mathrm{T}})$ was used in the TPC only analysis.

The raw p_{T} distribution of electrons, after the application of track selection criteria, is shown in Fig. 2 and is compared to the various background sources (charm hadron decays, photon conversions, Dalitz/di-electron decays, and hadron contamination) obtained from a MC simulation that included a description of the detector response. The p_{T} distributions of the background sources were normalized by the number of events which passed the event selection requirements, and were corrected for the efficiency to

Table 1: Contributions to the systematic uncertainty ($1<p_{\rm T}<8$ GeV/c) of the measurement of electrons from beauty hadron decays from the impact parameter method. The total systematic uncertainty is calculated as the quadrature sum of all contributions.

Uncertainty source	Systematic uncertainty (%)
Track matching	±2
ITS number of hits	±10
Number of TPC clusters for tracking	+1,-10(±1) for $p_{\rm T}<(>)$ 2 GeV/c
Number of TPC clusters for PID	±3
TOF PID	±3 for $p_{\rm T}<2$ GeV/c
TPC PID	±10
η and charge dependence	±2
minimum d_0 requirement	+15,-25(±15) for $p_{\rm T}<(>)$ 2 GeV/c
Light hadron decay background	$\approx$15 (<3) for $p_{\rm T}<(>)$ 2 GeV/c
Charm hadron decay background	+40, -60(<10) for $p_{\rm T}<(>)$ 2 GeV/c

reconstruct a primary collision vertex. Of those background contributions the Dalitz decay electrons and those from photon conversions are dominant at low $p_{\rm T}$, where more than 80% of the background can be attributed to π^0 Dalitz decays and conversions of photons from π^0 decays. At high $p_{\rm T}$ the contribution from charm hadron decays is important. The contribution from heavy quarkonia decays also becomes important at high $p_{\rm T}$, although they are considered negligible in this analysis as the selection on d_0 strongly suppresses tracks from such decays. The PYTHIA simulation does not precisely reproduce the $p_{\rm T}$-differential spectra of background sources measured in data. Therefore, the sources of background electrons simulated with PYTHIA were reweighted according to the π^0 $p_{\rm T}$ spectrum measured with ALICE [20] prior to propagation in the ALICE apparatus using GEANT3. The spectra of other light mesons was estimated via $m_{\rm T}$ scaling of the π^0 spectrum. The electron background from charm hadron decays were estimated based on the charm hadron spectra measured with ALICE. The D meson production cross sections were obtained by applying a $\sqrt{s}$ scaling to the cross sections measured at $\sqrt{s}$ = 7 TeV [21]. The scaling factor was defined as the ratio of the cross sections from the FONLL calculations at 2.76 and 7 TeV. The theoretical uncertainty on the scaling factor was evaluated by varying independently the quark mass and the perturbative scales as described in [22]. The D meson production cross sections were measured with ALICE, with limited precision and $p_{\rm T}$ coverage, in pp collisions at $\sqrt{s}$ = 2.76 TeV [6]. These measurements were found to be in agreement with the scaled 7 TeV measurements within statistical uncertainties. A contribution from $\Lambda_{\rm c}$ decays was included using the measured ratio $\sigma(\Lambda_{\rm c})/\sigma({\rm D}^0+{\rm D}^+)$ from ZEUS [23]. The background electrons surviving the selection criteria, including the condition on d_0, were subtracted from the inclusive electron distribution. The hadron contamination was estimated using a simultaneous fit of the electron and the different hadron components of the TPC dE/dx distribution in momentum slices. The contamination was negligible below 4 GeV/c but became significant towards higher momenta. At 8 GeV/c it was found to be approximately 7%. The contamination was statistically subtracted from the inclusive electron distribution. The resulting $p_{\rm T}$ distribution is shown as closed circles in Fig. 2.

The electron yield from beauty hadron decays was corrected for the geometrical acceptance, the track reconstruction efficiency, the electron identification efficiency, and the efficiency of the d_0 cut. The invariant cross section of electron production from beauty hadron decays in the range $|y| < 0.8$ was then calculated using the corrected electron $p_{\rm T}$ spectrum, the number of MB pp collisions and the MB cross section. The details are described in [17].

To evaluate the systematic uncertainties the analysis was repeated with modified track selection and

Particle IDentification (PID) criteria. The contributions to the systematic uncertainty are listed in Table 1. The systematic uncertainties due to the tracking efficiencies and the PID efficiencies amount to $^{+15}_{-18}(\pm 15)\%$ for $p_{\rm T} < 2$ GeV/c ($2 < p_{\rm T} < 6$ GeV/c). These reach $\approx ^{+20}_{-40}\%$ at 8 GeV/c due to the uncertainty of the hadron contamination subtraction. Additional contributions to the total systematic uncertainty include the d_0 requirement, evaluated by repeating the full analysis with modified selection criteria, and the subtraction of light flavor hadron decay background and charm hadron decay background, which were obtained by propagating the statistical and systematic uncertainties of the light flavor and charm hadron measurements used as analysis input. All systematic uncertainties specific to this analysis were added in quadrature to obtain the total systematic uncertainty.

3.2 Azimuthal electron-hadron correlation technique

The analysis is based on the shape of the distribution of the difference in azimuth ($\Delta\varphi$) between electrons and hadrons, and in particular of the peak at $\Delta\varphi$ around zero (near-side). Due to the mass difference of charm and beauty hadrons, the width of the near-side peak is larger for beauty compared to charm hadron decays. This method [24] has been used by the STAR experiment. A similar method based on the the invariant mass of like charge sign electron-kaon pairs [25] was used by the PHENIX experiment to extract a relative beauty contribution to the measured heavy-flavour electron production cross section.

The analysis was performed using the MB and EMCal trigger data sets. Electrons were selected in the range $1 < p_{\rm T} < 10$ GeV/c. For the MB analysis the selected electrons reached out to a transverse momentum of 6 GeV/c, while the analysis using EMCal triggered events selects electrons in the range $2.5 < p_{\rm T} < 10$ GeV/c.

The inclusive electron sample ($N_{\rm e_{incl}}$) contains electrons from heavy-flavour hadron decays and the aforementioned background sources, listed in Section 3.1. Di-electron pairs from photon conversions and π^0 Dalitz decays dominate at low $p_{\rm T}$ and were identified by pairing electrons with oppositely charged partner tracks and calculating the invariant mass ($M_{\rm e^+e^-}$) of each $\rm e^+e^-$ pair. The distribution for the background electrons is peaked at low $M_{\rm e^+e^-}$, while no correlation signal is present in the low $M_{\rm e^+e^-}$ region for the electrons from heavy-flavour decays. These unlike charge-sign (ULS) pairs contain true conversion and Dalitz decay electrons, along with a small fraction of heavy-flavour electrons that were wrongly paired with a background electron. The latter can be identified by calculating the invariant mass of like charge-sign (LS) pairs. Using a MC simulation with GEANT3, where pp collisions are generated using PYTHIA 6 (Perugia-0 tune) and by comparing the ULS and LS invariant mass distribution the selection criteria on $M_{\rm e^+e^-}$, identical for the LS and ULS pairs, were determined. Electrons with $M_{\rm e^+e^-} < 50(100)$ MeV/c^2 for the EMCal(MB) analysis were identified as background. The background finding efficiency (ε) ranges from $\sim 20\%$ at low $p_{\rm T}$ to $\sim 66\%$ for $p_{\rm T}$ above 4 GeV/c.

The number of heavy-flavour hadron decay electrons can be expressed as

$$N_{\rm e_{HF}} = N_{\rm e_{incl}} - \frac{1}{\varepsilon}\left(N_{\rm e_{ULS}} - N_{\rm e_{LS}}\right), \tag{1}$$

where $N_{\rm e_{ULS}}$ ($N_{\rm e_{LS}}$) are the number of electrons which formed a ULS(LS) pair with a $M_{\rm e^+e^-}$ satisfying the previously mentioned selection criteria. Each electron contribution from Equation (1) is taken, along with the charged hadrons in the event and the heavy-flavour decay electron-hadron azimuthal correlation distribution, $\frac{1}{N_{\rm e}}\left(\frac{{\rm d}N}{{\rm d}\Delta\varphi}\right)_{\rm e-h}$, was constructed.

To determine the fraction of electrons from beauty hadron decays the measured azimuthal e-h correlation distribution was fit with the function

$$\frac{1}{N_{\rm e}}\left(\frac{{\rm d}N}{{\rm d}\Delta\varphi}\right)_{\rm e-h} = C + r_{\rm b}\frac{1}{N_{\rm e_b}}\left(\frac{{\rm d}N}{{\rm d}\Delta\varphi}\right)_{\rm e_b-h} + (1-r_{\rm b})\frac{1}{N_{\rm e_c}}\left(\frac{{\rm d}N}{{\rm d}\Delta\varphi}\right)_{\rm e_c-h}, \tag{2}$$

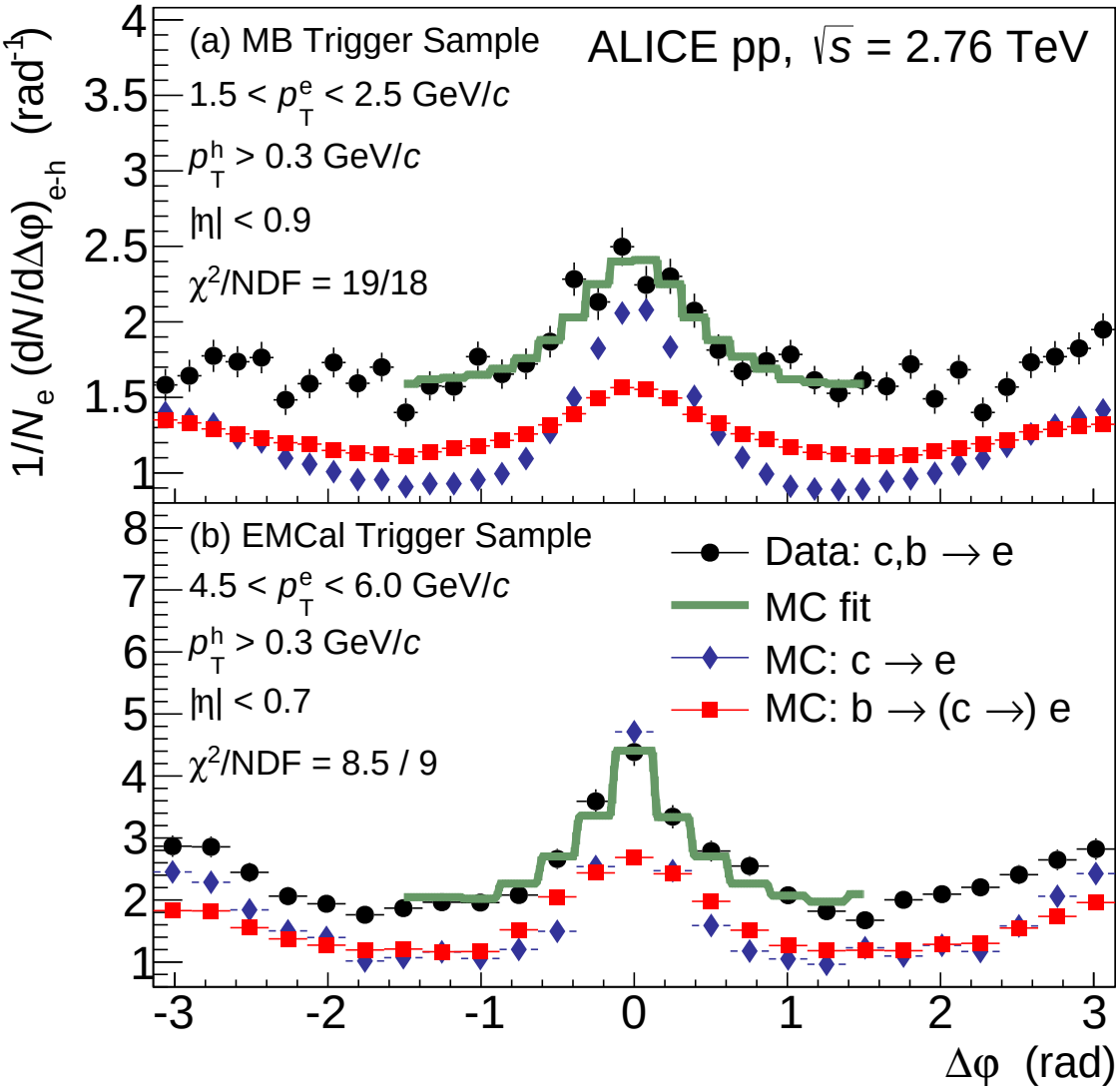

Fig. 3: (Color online) The azimuthal correlation between heavy-flavour decay electrons and charged hadrons, scaled by the number of electrons is shown for (a) the MB events in the p_T^e range 1.5-2.5 GeV/c and (b) the EMCal events in the p_T^e range 4.5-6.0 GeV/c. The diamonds represent the MC distribution for electrons from charm hadron decays, squares are the MC distribution for electrons from beauty hadrons decays. The line is the MC fit (Eq. 2) to the data points (circles).

Table 2: Contributions to the systematic uncertainty of the fraction of electrons from beauty to the total number of electrons from heavy-flavour decays measured using the e-h azimuthal correlation technique. The total systematic uncertainty is calculated as the quadrature sum of all contributions.

Event trigger	MB	EMCal
Uncertainty source	Systematic uncertainty (%)	
Number of TPC clusters for tracking	$\pm$8	5
TPC PID	$\pm$5(+5,-20) for p_{T}<(>)3.5 GeV/c	$\pm$5($\pm$10) for p_{T}<(>)3.5 GeV/c
TOF PID	$\pm$5	n.a.
EMCal PID	n.a.	$\pm$10($\pm$5) for p_{T}<(>)3.5 GeV/c
e^+e^- invariant mass	negligible	$\pm$10($\pm$5) for p_{T}<(>)3.5 GeV/c
Associated electron PID	$\pm$1	$\pm$1($\pm$5) for p_{T}<(>)4.5 GeV/c
Associated hadron momentum	$\pm$8	$\pm$10($\pm$5) for p_{T}<(>)3.5 GeV/c
Fit range	negligible	negligible($\pm$5) for p_{T}<(>6) GeV/c
Light hadron decay background	$\pm$1	$\pm$25($\pm$5) for p_{T}<(>)3.5 GeV/c

where r_b, a free parameter of the fit, is the fraction of electrons from beauty to the total number of electrons from all heavy-flavour decays, $\Delta\varphi$ is the azimuthal angle between the electron and the charged hadron. The distributions of the azimuthal correlations $\left(\frac{\mathrm{d}N}{\mathrm{d}\Delta\varphi}\right)_{\mathrm{e_{b(c)}-h}}$ for electrons from beauty (charm) hadron decays were taken from the previously mentioned MC simulation, and the constant C accounts for the uncorrelated background. Fig. 3 shows the measured azimuthal correlation, scaled by the number of electrons, along with the MC fit templates and the full fit for both (a) the MB and (b) the EMCal trigger analyses, in the p_{T} range of 1.5-2.5 GeV/c and 4.5-6 GeV/c, respectively. For each p_{T} bin the measured distribution was fit over the range $|\Delta\varphi| < 1.5$ rad. From the fit the relative beauty fraction (r_b) is extracted as a function of p_{T}. The values of r_b obtained from the MB and EMCal triggered samples were found to agree within the systematic and statistical uncertainties in the overlapping p_{T} intervals. Hence, in the common p_{T} range, the final results for the relative beauty contribution to heavy-flavour decay electrons was obtained as the weighted average of the results from the MB and EMCal samples.

The main sources of systematic uncertainty include the electron identification selection criteria and the background finding efficiency. As previously explained, the background electrons were identified using invariant mass $M_{\mathrm{e^+e^-}}$. The selected mass requirement, as a source of systematic uncertainty was found to be negligible for the MB analysis and reached a maximum of 10% for $p_{\mathrm{T}} < 3.5$ GeV for the EMCal analysis. The efficiency of the invariant mass method was calculated using a MC sample. For the EMCal analysis a MC simulation enhanced with π^0 and η mesons, flat in p_{T}, was used in order to properly estimate the background finding efficiency at high p_{T}, as the MB MC sample did not provide enough statistics. The bias from the enhancement is corrected by reweighting to obtain the correct p_{T} distribution of the π^0 (see Section 3.1). Overall, the systematic uncertainties range from 9-21% for the MB analysis and from 12-33% in the case of the EMCal analysis, depending on the transverse momentum. The final systematic uncertainties were obtained by combining these two measurements, yielding 17% for the lower momentum region ($p_{\mathrm{T}} < 3.5$ GeV/c) and $^{+16}_{-25}$% for the higher momentum region ($3.5 < p_{\mathrm{T}} < 10$ GeV/c). All systematic uncertainties are listed in Table 2.

For the MB analysis the hadron contamination to the electron sample was estimated using a simultaneous fit of the electron and the different hadron components of the TPC dE/dx distribution in momentum ranges, while for the EMCal analysis the contamination was estimated using a fit to the E/p distribution in momentum slices. The contamination was found to be negligible for $p_{\mathrm{T}} < 4(6)$ GeV/c for the MB(EMCal) analysis. For the highest p_{T} of the MB analysis the contamination was 5% and reached 20% for the highest p_{T} of the EMCal analysis. No subtraction of this contamination was performed. Instead it is taken into account in the PID systematic uncertainties. In addition, a mixed event technique was used to cross-check that detector acceptance effects are well reproduced in the MC sample. For the mixed event $\Delta\varphi$ correlation distribution, electrons from EMCal trigger events and hadrons from the

MB sample were selected. Hadrons were selected only from MB events to remove the bias from EMCal trigger sample in the correlation distribution from mixed event. The mixed event correlation distribution was found to be flat over the entire $\Delta\varphi$ range, implying that detector effects do not bias the correlation distribution. Hence a mixed event correction was not applied to the resulting $\Delta\varphi$ distribution.

4 Results

The relative beauty contribution to heavy-flavour decay electrons obtained from the impact parameter analysis along with that extracted from the azimuthal correlation method, as a function of p_{T} is shown in Fig. 4(a). For the impact parameter analysis the beauty contribution to the heavy-flavour electron spectrum was measured, while the charm contribution was calculated from the charm hadron spectra measured by ALICE as described in Section 3.1. Within the statistical and systematic uncertainties the resulting fractions are in agreement with each other and show that the beauty contribution to the total heavy-flavour spectrum is comparable to the contribution from charm for $p_{\mathrm{T}} > 4$ GeV/c.

The measurements are compared to the central, upper, and lower predictions of three pQCD calculations [1, 10, 3], represented by the various lines. The central values of the fraction of electrons from beauty hadron decays was calculated using the central values of the beauty and charm to electron cross sections. The upper (lower) predictions were obtained by calculating the beauty fraction using the upper (lower) uncertainty limit of the beauty to electron cross section and the lower (upper) limit of the charm to electron cross section. The upper and lower lines demonstrate the uncertainty range of the calculations, which originate from the variation of the perturbative scales and the heavy quark masses as described in [1, 2, 3]. Each prediction describes the relative beauty contribution fraction over the whole p_{T} range.

The p_{T}-differential cross section of electrons from beauty decays measured using the impact parameter analysis is shown in Fig. 4 (b) and it is compared to the spectrum obtained using the beauty fraction from the e-h correlation analysis and the measured heavy-flavour decay electron cross section from [7]. This alternative approach agrees with the result obtained using the impact parameter technique. As the resulting spectrum obtained using the impact parameter based analysis ($|y| < 0.8$) yielded finer p_{T} intervals and smaller uncertainties this result for $p_{\mathrm{T}} < 8$ GeV/c is used with the higher p_{T} slice of the e-h correlation analysis ($|y| < 0.7$) to obtain the total beauty production cross section.

The measured p_{T}-differential cross section, obtained using the impact parameter analysis for $p_{\mathrm{T}} < 8$ GeV/c and including the highest p_{T} point from the correlation analysis, in the p_{T} range 1-10 GeV/c is shown in Fig. 5 (a) along with a comparison to the upper and lower uncertainty limits of the aforementioned pQCD calculations. Fig. 5 (b)-(d) shows the ratio of the data to the central theoretical predictions. The data and predictions are consistent within the experimental and theoretical uncertainties. Due to the uncertainty of the measured luminosity all measured cross sections have an additional normalization uncertainty of 1.9% [13].

The visible cross section of electrons from beauty hadron decays at mid-rapidity ($|y| < 0.8$) was obtained by integrating the p_{T}-differential cross section in the measured p_{T} range ($1 < p_{\mathrm{T}} < 10$ GeV/c), obtaining $\sigma_{\mathrm{b}\to\mathrm{e}} = 3.47 \pm 0.40(\mathrm{stat})^{+1.12}_{-1.33}(\mathrm{sys}) \pm 0.07(\mathrm{norm})$ μb. The visible cross section is then scaled by the ratio of the total cross section of electrons originating from beauty hadron decays from FONLL in the full p_{T} range to the FONLL cross section integrated in the measured p_{T} range. The central value of the extrapolation factor was computed using the FONLL prediction with the central values of the quark mass and perturbative scale. The uncertainties were obtained by varying the quark mass and perturbative scale and recalculating the ratio, which is given separately in the results as extrapolation uncertainty. For the extrapolation the beauty hadron to electron branching ratio of $\mathrm{BR}_{\mathrm{H_b}\to\mathrm{e}} + \mathrm{BR}_{\mathrm{H_b}\to\mathrm{H_c}\to\mathrm{e}} = 0.205 \pm 0.007$ [26] is used.

The cross section of electrons from beauty hadron decays at mid-rapidity, $\frac{\mathrm{d}\sigma_{\mathrm{b\bar{b}}}}{\mathrm{d}y} = 23.28 \pm 2.70(\mathrm{stat})^{+8.92}_{-8.70}$

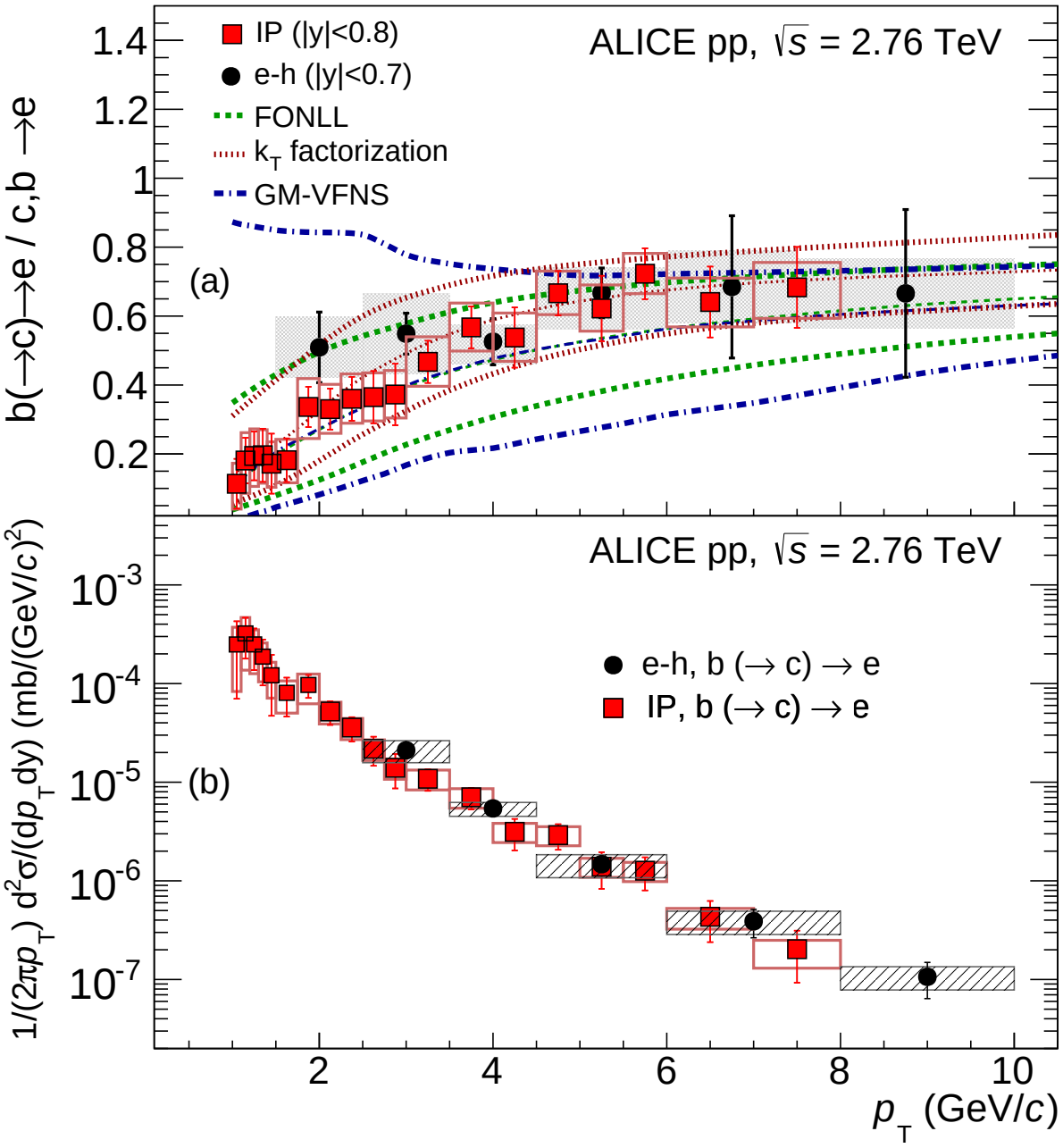

Fig. 4: (Color online) (a) Relative beauty contribution to the heavy-flavour electron yield; measured from the azimuthal correlations between heavy-flavour decay electrons and charged hadrons (black circles) compared to that from the method based on the track impact parameter (red squares). The green dashed, red dotted, and blue dot-dashed lines represent the FONLL, k_{T}-factorization, and GM-VFNS predictions, respectively. (b) The b ($\rightarrow$ c) $\rightarrow$ e p_{T}-differential cross section obtained using the impact parameter method (red squares) and the e-h correlation (black circles) method. For both panels, the error bars (boxes) represent the statistical (systematic) uncertainties.

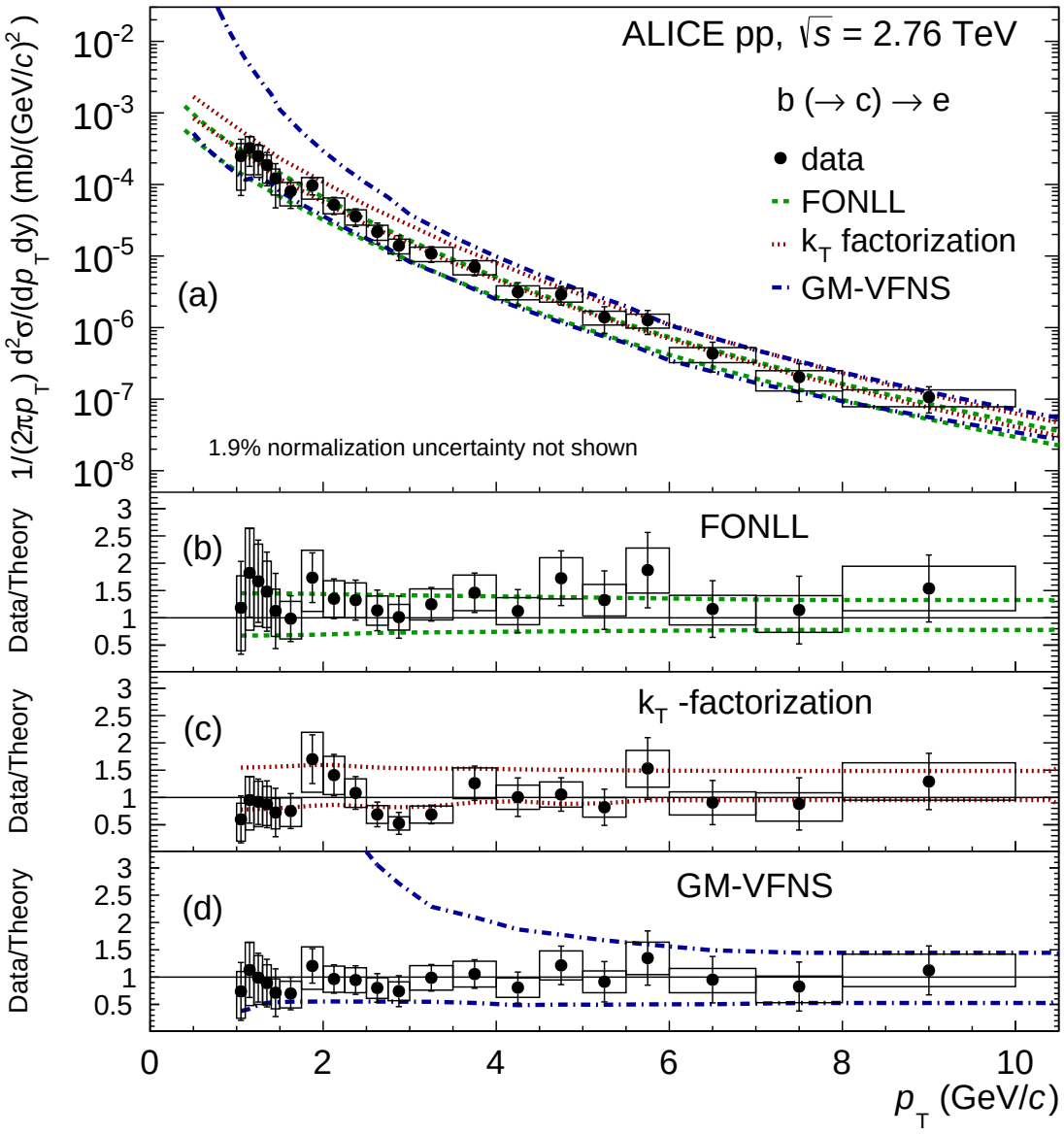

Fig. 5: (Color online) (a) p_{T}-differential invariant cross section of electrons from beauty hadron decays. The green dashed, red dotted, and blue dot-dashed lines represent the FONLL, k_{T}-factorization, and GM-VFNS uncertainty range, respectively. (b)-(d) Ratios of the data and the central prediction of pQCD calculations for electrons from beauty hadron decays. For all panels, the error bars (boxes) represent the statistical (systematic) uncertainties

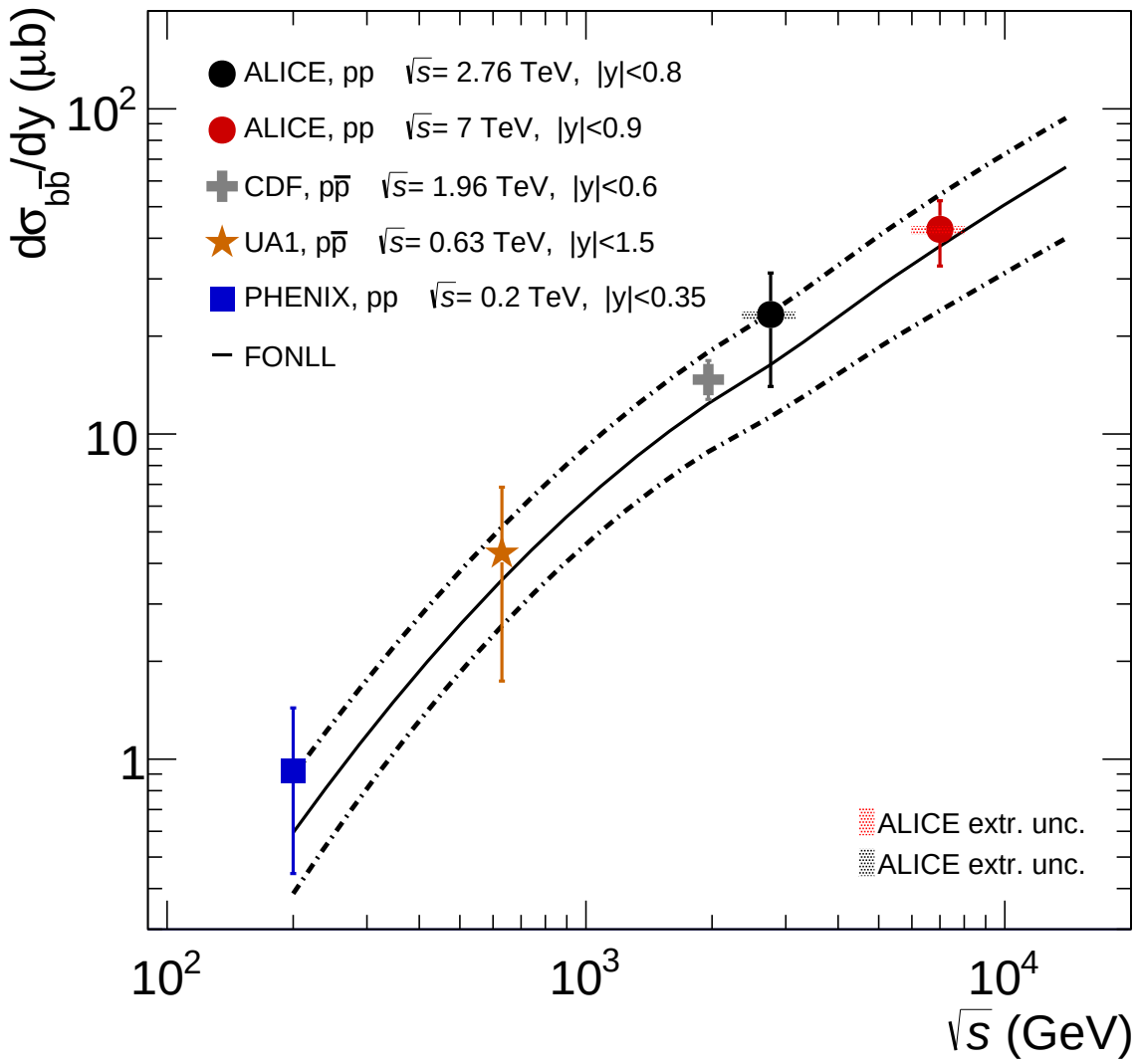

Fig. 6: (Color online) Beauty production cross section per rapidity unit measured at mid-rapidity as a function of center of mass energy in pp collisions (PHENIX [25] and ALICE [17] results) and $\mathrm{p\bar{p}}$ collisions (UA1 [28] and CDF [27] results) along with the comparison to FONLL calculations. Error bars represent the statistical and systematic uncertainties added in quadrature.

$(\mathrm{sys})^{+0.49}_{-0.65}(\mathrm{extr}) \pm 0.44(\mathrm{norm})$ μb, is shown in Fig. 6 as a function of center of mass energy for experimental measurements [25, 27, 28], including the result obtained by ALICE at 7 TeV [17]. The total beauty production cross section was obtained in an analogous way and is found to be $\sigma_{\mathrm{b\bar{b}}} = 130 \pm 15.1(\mathrm{stat})^{+42.1}_{-49.8}(\mathrm{sys})^{+3.4}_{-3.1}(\mathrm{extr}) \pm 2.5(\mathrm{norm}) \pm 4.4(\mathrm{BR})$ μb. The corresponding prediction of FONLL is $\sigma_{\mathrm{b\bar{b}}} = 95.5^{+139}_{-66.5}$ μb.

5 Summary

The invariant production cross section of electrons from semi-leptonic decays of beauty hadrons is reported at mid-rapidity ($|y| < 0.8$) in the transverse momentum range $1 < p_{\mathrm{T}} < 10$ GeV/c in pp collisions at $\sqrt{s}$ = 2.76 TeV. The measurement extending to a p_{T} of 8 GeV/c was performed using a selection of tracks based on their impact parameter to identify displaced electrons from beauty hadron decays.

An alternative method, which utilized the measured electron-hadron azimuthal correlations extended the p_{T} range up to 10 GeV/c, and was found to be in agreement with the results from the impact parameter method. The results were compared to various pQCD calculations and compatibility between data and theory was found. The integrated visible cross section is $\sigma_{\mathrm{b}\rightarrow\mathrm{e}} = 3.47 \pm 0.40(\mathrm{stat})^{+1.12}_{-1.33}(\mathrm{sys}) \pm 0.07(\mathrm{norm})\ \mu\mathrm{b}$, and was extrapolated to full phase space using FONLL to obtain the total $\mathrm{b\bar{b}}$ production cross section, $\sigma_{\mathrm{b\bar{b}}} = 130 \pm 15.1(\mathrm{stat})^{+42.1}_{-49.8}(\mathrm{sys})^{+3.4}_{-3.1}(\mathrm{extr}) \pm 2.5(\mathrm{norm}) \pm 4.4(\mathrm{BR})\ \mu\mathrm{b}$. Furthermore, these results provide a crucial baseline for the study of beauty quark production in Pb-Pb collisions at the LHC.

Acknowledgements

The ALICE Collaboration would like to thank all its engineers and technicians for their invaluable contributions to the construction of the experiment and the CERN accelerator teams for the outstanding performance of the LHC complex.
The ALICE Collaboration gratefully acknowledges the resources and support provided by all Grid centres and the Worldwide LHC Computing Grid (WLCG) collaboration.
The ALICE Collaboration acknowledges the following funding agencies for their support in building and running the ALICE detector:
State Committee of Science, World Federation of Scientists (WFS) and Swiss Fonds Kidagan, Armenia, Conselho Nacional de Desenvolvimento Científico e Tecnológico (CNPq), Financiadora de Estudos e Projetos (FINEP), Fundação de Amparo à Pesquisa do Estado de São Paulo (FAPESP);
National Natural Science Foundation of China (NSFC), the Chinese Ministry of Education (CMOE) and the Ministry of Science and Technology of China (MSTC);
Ministry of Education and Youth of the Czech Republic;
Danish Natural Science Research Council, the Carlsberg Foundation and the Danish National Research Foundation;
The European Research Council under the European Community's Seventh Framework Programme;
Helsinki Institute of Physics and the Academy of Finland;
French CNRS-IN2P3, the 'Region Pays de Loire', 'Region Alsace', 'Region Auvergne' and CEA, France;
German BMBF and the Helmholtz Association;
General Secretariat for Research and Technology, Ministry of Development, Greece;
Hungarian OTKA and National Office for Research and Technology (NKTH);
Department of Atomic Energy and Department of Science and Technology of the Government of India;
Istituto Nazionale di Fisica Nucleare (INFN) and Centro Fermi - Museo Storico della Fisica e Centro Studi e Ricerche "Enrico Fermi", Italy;
MEXT Grant-in-Aid for Specially Promoted Research, Japan;
Joint Institute for Nuclear Research, Dubna;
National Research Foundation of Korea (NRF);
CONACYT, DGAPA, México, ALFA-EC and the EPLANET Program (European Particle Physics Latin American Network)
Stichting voor Fundamenteel Onderzoek der Materie (FOM) and the Nederlandse Organisatie voor Wetenschappelijk Onderzoek (NWO), Netherlands;
Research Council of Norway (NFR);
Polish Ministry of Science and Higher Education;
National Science Centre, Poland;
Ministry of National Education/Institute for Atomic Physics and CNCS-UEFISCDI - Romania;
Ministry of Education and Science of Russian Federation, Russian Academy of Sciences, Russian Federal Agency of Atomic Energy, Russian Federal Agency for Science and Innovations and The Russian Foundation for Basic Research;
Ministry of Education of Slovakia;

Department of Science and Technology, South Africa;
CIEMAT, EELA, Ministerio de Economía y Competitividad (MINECO) of Spain, Xunta de Galicia (Consellería de Educación), CEADEN, Cubaenergía, Cuba, and IAEA (International Atomic Energy Agency);
Swedish Research Council (VR) and Knut & Alice Wallenberg Foundation (KAW);
Ukraine Ministry of Education and Science;
United Kingdom Science and Technology Facilities Council (STFC);
The United States Department of Energy, the United States National Science Foundation, the State of Texas, and the State of Ohio.

References

[1] M. Cacciari, S. Frixione, N. Houdeau, M. L. Mangano, P. Nason, et al., Theoretical predictions for charm and bottom production at the LHC, JHEP 1210 (2012) 137.

[2] B. Kniehl, G. Kramer, I. Schienbein, H. Spiesberger, Inclusive Charmed-Meson Production at the CERN LHC, Eur.Phys.J. C72 (2012) 2082.

[3] R. Maciula, A. Szczurek, Open charm production at the LHC - k_t-factorization approach, Phys.Rev. D87 (9) (2013) 094022.

[4] B. Abelev, et al., Suppression of high transverse momentum D mesons in central Pb-Pb collisions at $\sqrt{s_{NN}} = 2.76$ TeV, JHEP 1209 (2012) 112.

[5] B. Abelev, et al., D meson elliptic flow in non-central Pb-Pb collisions at $\sqrt{s_{NN}} = 2.76$ TeV, Phys.Rev.Lett. 111 (2013) 102301.

[6] B. Abelev, et al., Measurement of charm production at central rapidity in proton–proton collisions at $\sqrt{s} = 2.76$ TeV, JHEP 1207 191.

[7] B. Abelev, et al., Measurement of electrons from semileptonic heavy-flavor hadron decays in pp collisions at $\sqrt{s} = 2.76$ TeV, to be published, ArXiv:14xx.xxxx [nucl-ex].

[8] B. Abelev, et al., Production of Muons from Heavy Flavor Decays at Forward Rapidity in pp and Pb-Pb Collisions at $\sqrt{s_{NN}} = 2.76$ TeV, Phys. Rev. Lett. 109 (2012) 112301.

[9] B. Abelev, et al., Inclusive J/ψ production in pp collisions at $\sqrt{s} = 2.76$ TeV, Phys.Lett. B718 (2012) 295.

[10] P. Bolzoni, G. Kramer, Inclusive lepton production from heavy-hadron decay in pp collisions at the LHC, Nucl.Phys. B872 (2013) 253.

[11] K. Aamodt, et al., The ALICE experiment at the CERN LHC, JINST 3 (2008) S08002.

[12] B. Abelev, et al., Performance of the ALICE Experiment at the CERN LHC, ArXiv:1402.4476 [nucl-ex].

[13] B. Abelev, et al., Measurement of inelastic, single- and double-diffraction cross sections in proton–proton collisions at the LHC with ALICE, Eur.Phys.J. C73 (2013) 2456.

[14] J. Kral, T. Awes, H. Muller, J. Rak, J. Schambach, L0 trigger for the EMCal detector of the ALICE experiment, Nucl.Instrum.Meth. A693 (2012) 261.

[15] J. Alme, et al., The ALICE TPC, a large 3-dimensional tracking device with fast readout for ultra-high multiplicity events, Nucl.Instrum.Meth. A622 (2010) 316.

[16] K. Aamodt, et al., Alignment of the ALICE Inner Tracking System with cosmic-ray tracks, JINST 5 (2010) P03003.

[17] B. Abelev, et al., Measurement of electrons from beauty hadron decays in pp collisions at $\sqrt{s} = 7$ TeV, Phys.Lett. B721 (2013) 13.

[18] R. Brun, et al., CERN Program Library Long Write-up, W5013 (1994).

[19] P. Z. Skands, The Perugia Tunes, ArXiv:0905.3418 [hep-ph].

[20] B. Abelev, et al., Neutral pion production at midrapidity in pp and PbPb collisions at $\sqrt{s_{NN}} = 2.76$ TeV, to be published, ArXiv:14xx.xxxx [nucl-ex].

[21] K. Aamodt, et al., Measurement of charm production at central rapidity in proton–proton collisions at $\sqrt{s} = 7$ TeV, JHEP 01 (2012) 128.

[22] R. Averbeck, N. Bastid, Z. C. del Valle, P. Crochet, A. Dainese, et al., Reference Heavy Flavour Cross Sections in pp Collisions at $\sqrt{s}$ = 2.76 TeV, using a pQCD-Driven $\sqrt{s}$-Scaling of ALICE Measurements at $\sqrt{s}$ = 7 TeV, ArXiv:1107.3243 [hep-ph].

[23] S. Chekanov, et al., Measurement of charm fragmentation ratios and fractions in photoproduction at HERA, Eur. Phys. J. C44 (2005) 351.

[24] M. Aggarwal, et al., Measurement of the Bottom contribution to non-photonic electron production in pp collisions at $\sqrt{s}$=200 GeV, Phys.Rev.Lett. 105 (2010) 202301.

[25] A. Adare, et al., Measurement of Bottom versus Charm as a Function of Transverse Momentum with Electron-Hadron Correlations in pp Collisions at $\sqrt{s}$=200 GeV, Phys.Rev.Lett. 103 (2009) 082002.

[26] J. Beringer, et al., The Review of Particle Physics, Phys. Rev. D86 (2012) 010001.

[27] D. Acosta, et al., Measurement of the J/ψ meson and $b-$hadron production cross sections in $p\bar{p}$ collisions at $\sqrt{s} = 1960$ GeV, Phys. Rev. D71 (2005) 032001.

[28] C. Albajar, et al., Beauty production at the CERN p anti-p collider, Phys.Lett. B256 (1991) 121.

A The ALICE Collaboration

B. Abelev[69] , J. Adam[37] , D. Adamová[77] , M.M. Aggarwal[81] , M. Agnello[105 ,88] , A. Agostinelli[26] , N. Agrawal[44] , Z. Ahammed[124] , N. Ahmad[18] , I. Ahmed[15] , S.U. Ahn[62] , S.A. Ahn[62] , I. Aimo[105 ,88] , S. Aiola[129] , M. Ajaz[15] , A. Akindinov[53] , S.N. Alam[124] , D. Aleksandrov[94] , B. Alessandro[105] , D. Alexandre[96] , A. Alici[12 ,99] , A. Alkin[3] , J. Alme[35] , T. Alt[39] , S. Altinpinar[17] , I. Altsybeev[123] , C. Alves Garcia Prado[113] , C. Andrei[72] , A. Andronic[91] , V. Anguelov[87] , J. Anielski[49] , T. Antičić[92] , F. Antinori[102] , P. Antonioli[99] , L. Aphecetche[107] , H. Appelshäuser[48] , S. Arcelli[26] , N. Armesto[16] , R. Arnaldi[105] , T. Aronsson[129] , I.C. Arsene[91] , M. Arslandok[48] , A. Augustinus[34] , R. Averbeck[91] , T.C. Awes[78] , M.D. Azmi[83] , M. Bach[39] , A. Badalà[101] , Y.W. Baek[64 ,40] , S. Bagnasco[105] , R. Bailhache[48] , R. Bala[84] , A. Baldisseri[14] , F. Baltasar Dos Santos Pedrosa[34] , R.C. Baral[56] , R. Barbera[27] , F. Barile[31] , G.G. Barnaföldi[128] , L.S. Barnby[96] , V. Barret[64] , J. Bartke[110] , M. Basile[26] , N. Bastid[64] , S. Basu[124] , B. Bathen[49] , G. Batigne[107] , A. Batista Camejo[64] , B. Batyunya[61] , P.C. Batzing[21] , C. Baumann[48] , I.G. Bearden[74] , H. Beck[48] , C. Bedda[88] , N.K. Behera[44] , I. Belikov[50] , F. Bellini[26] , R. Bellwied[115] , E. Belmont-Moreno[59] , R. Belmont III[127] , V. Belyaev[70] , G. Bencedi[128] , S. Beole[25] , I. Berceanu[72] , A. Bercuci[72] , Y. Berdnikov[,ii,79] , D. Berenyi[128] , M.E. Berger[86] , R.A. Bertens[52] , D. Berzano[25] , L. Betev[34] , A. Bhasin[84] , I.R. Bhat[84] , A.K. Bhati[81] , B. Bhattacharjee[41] , J. Bhom[120] , L. Bianchi[25] , N. Bianchi[66] , C. Bianchin[52] , J. Bielčík[37] , J. Bielčíková[77] , A. Bilandzic[74] , S. Bjelogrlic[52] , F. Blanco[10] , D. Blau[94] , C. Blume[48] , F. Bock[87 ,68] , A. Bogdanov[70] , H. Bøggild[74] , M. Bogolyubsky[106] , F.V. Böhmer[86] , L. Boldizsár[128] , M. Bombara[38] , J. Book[48] , H. Borel[14] , A. Borissov[90 ,127] , F. Bossú[60] , M. Botje[75] , E. Botta[25] , S. Böttger[47] , P. Braun-Munzinger[91] , M. Bregant[113] , T. Breitner[47] , T.A. Broker[48] , T.A. Browning[89] , M. Broz[37] , E. Bruna[105] , G.E. Bruno[31] , D. Budnikov[93] , H. Buesching[48] , S. Bufalino[105] , P. Buncic[34] , O. Busch[87] , Z. Buthelezi[60] , D. Caffarri[28] , X. Cai[7] , H. Caines[129] , L. Calero Diaz[66] , A. Caliva[52] , E. Calvo Villar[97] , P. Camerini[24] , F. Carena[34] , W. Carena[34] , J. Castillo Castellanos[14] , E.A.R. Casula[23] , V. Catanescu[72] , C. Cavicchioli[34] , C. Ceballos Sanchez[9] , J. Cepila[37] , P. Cerello[105] , B. Chang[116] , S. Chapeland[34] , J.L. Charvet[14] , S. Chattopadhyay[124] , S. Chattopadhyay[95] , V. Chelnokov[3] , M. Cherney[80] , C. Cheshkov[122] , B. Cheynis[122] , V. Chibante Barroso[34] , D.D. Chinellato[115] , P. Chochula[34] , M. Chojnacki[74] , S. Choudhury[124] , P. Christakoglou[75] , C.H. Christensen[74] , P. Christiansen[32] , T. Chujo[120] , S.U. Chung[90] , C. Cicalo[100] , L. Cifarelli[26 ,12] , F. Cindolo[99] , J. Cleymans[83] , F. Colamaria[31] , D. Colella[31] , A. Collu[23] , M. Colocci[26] , G. Conesa Balbastre[65] , Z. Conesa del Valle[46] , M.E. Connors[129] , J.G. Contreras[11] , T.M. Cormier[127] , Y. Corrales Morales[25] , P. Cortese[30] , I. Cortés Maldonado[2] , M.R. Cosentino[113] , F. Costa[34] , P. Crochet[64] , R. Cruz Albino[11] , E. Cuautle[58] , L. Cunqueiro[66] , A. Dainese[102] , R. Dang[7] , A. Danu[57] , D. Das[95] , I. Das[46] , K. Das[95] , S. Das[4] , A. Dash[114] , S. Dash[44] , S. De[124] , H. Delagrange[107 ,i] , A. Deloff[71] , E. Dénes[128] , G. D'Erasmo[31] , A. De Caro[29 ,12] , G. de Cataldo[98] , J. de Cuveland[39] , A. De Falco[23] , D. De Gruttola[29 ,12] , N. De Marco[105] , S. De Pasquale[29] , R. de Rooij[52] , M.A. Diaz Corchero[10] , T. Dietel[49] , P. Dillenseger[48] , R. Divià[34] , D. Di Bari[31] , S. Di Liberto[103] , A. Di Mauro[34] , P. Di Nezza[66] , Ø. Djuvsland[17] , A. Dobrin[52] , T. Dobrowolski[71] , D. Domenicis Gimenez[113] , B. Dönigus[48] , O. Dordic[21] , S. Dørheim[86] , A.K. Dubey[124] , A. Dubla[52] , L. Ducroux[122] , P. Dupieux[64] , A.K. Dutta Majumdar[95] , T. E. Hilden[42] , R.J. Ehlers[129] , D. Elia[98] , H. Engel[47] , B. Erazmus[34 ,107] , H.A. Erdal[35] , D. Eschweiler[39] , B. Espagnon[46] , M. Esposito[34] , M. Estienne[107] , S. Esumi[120] , D. Evans[96] , S. Evdokimov[106] , D. Fabris[102] , J. Faivre[65] , D. Falchieri[26] , A. Fantoni[66] , M. Fasel[87] , D. Fehlker[17] , L. Feldkamp[49] , D. Felea[57] , A. Feliciello[105] , G. Feofilov[123] , J. Ferencei[77] , A. Fernández Téllez[2] , E.G. Ferreiro[16] , A. Ferretti[25] , A. Festanti[28] , J. Figiel[110] , M.A.S. Figueredo[117] , S. Filchagin[93] , D. Finogeev[51] , F.M. Fionda[31] , E.M. Fiore[31] , E. Floratos[82] , M. Floris[34] , S. Foertsch[60] , P. Foka[91] , S. Fokin[94] , E. Fragiacomo[104] , A. Francescon[34 ,28] , U. Frankenfeld[91] , U. Fuchs[34] , C. Furget[65] , M. Fusco Girard[29] , J.J. Gaardhøje[74] , M. Gagliardi[25] , A.M. Gago[97] , M. Gallio[25] , D.R. Gangadharan[19] , P. Ganoti[78] , C. Garabatos[91] , E. Garcia-Solis[13] , C. Gargiulo[34] , I. Garishvili[69] , J. Gerhard[39] , M. Germain[107] , A. Gheata[34] , M. Gheata[34 ,57] , B. Ghidini[31] , P. Ghosh[124] , S.K. Ghosh[4] , P. Gianotti[66] , P. Giubellino[34] , E. Gladysz-Dziadus[110] , P. Glässel[87] , A. Gomez Ramirez[47] , P. González-Zamora[10] , S. Gorbunov[39] , L. Görlich[110] , S. Gotovac[109] , L.K. Graczykowski[126] , A. Grelli[52] , A. Grigoras[34] , C. Grigoras[34] , V. Grigoriev[70] , A. Grigoryan[1] , S. Grigoryan[61] , B. Grinyov[3] , N. Grion[104] , J.F. Grosse-Oetringhaus[34] , J.-Y. Grossiord[122] , R. Grosso[34] , F. Guber[51] , R. Guernane[65] , B. Guerzoni[26] , M. Guilbaud[122] , K. Gulbrandsen[74] , H. Gulkanyan[1] , M. Gumbo[83] , T. Gunji[119] , A. Gupta[84] , R. Gupta[84] , K. H. Khan[15] , R. Haake[49] , Ø. Haaland[17] , C. Hadjidakis[46] , M. Haiduc[57] , H. Hamagaki[119] , G. Hamar[128] , L.D. Hanratty[96] , A. Hansen[74] , J.W. Harris[129] , H. Hartmann[39] , A. Harton[13] , D. Hatzifotiadou[99] , S. Hayashi[119] , S.T. Heckel[48] , M. Heide[49] , H. Helstrup[35] , A. Herghelegiu[72] , G. Herrera Corral[11] , B.A. Hess[33] , K.F. Hetland[35] , B. Hippolyte[50] , J. Hladky[55] , P. Hristov[34] , M. Huang[17] , T.J. Humanic[19] , N. Hussain[41] , D. Hutter[39] , D.S. Hwang[20] , R. Ilkaev[93] , I. Ilkiv[71] , M. Inaba[120] , G.M. Innocenti[25] , C. Ionita[34] , M. Ippolitov[94] , M. Irfan[18] , M. Ivanov[91] , V. Ivanov[79] , A. Jachołkowski[27] , P.M. Jacobs[68] , C. Jahnke[113] , H.J. Jang[62] , M.A. Janik[126] , P.H.S.Y. Jayarathna[115] , C. Jena[28] , S. Jena[115] ,

R.T. Jimenez Bustamante[58] , P.G. Jones[96] , H. Jung[40] , A. Jusko[96] , V. Kadyshevskiy[61] , S. Kalcher[39] , P. Kalinak[54] , A. Kalweit[34] , J. Kamin[48] , J.H. Kang[130] , V. Kaplin[70] , S. Kar[124] , A. Karasu Uysal[63] , O. Karavichev[51] , T. Karavicheva[51] , E. Karpechev[51] , U. Kebschull[47] , R. Keidel[131] , D.L.D. Keijdener[52] , M.M. Khan[iii,18] , P. Khan[95] , S.A. Khan[124] , A. Khanzadeev[79] , Y. Kharlov[106] , B. Kileng[35] , B. Kim[130] , D.W. Kim[62,40] , D.J. Kim[116] , J.S. Kim[40] , M. Kim[40] , M. Kim[130] , S. Kim[20] , T. Kim[130] , S. Kirsch[39] , I. Kisel[39] , S. Kiselev[53] , A. Kisiel[126] , G. Kiss[128] , J.L. Klay[6] , J. Klein[87] , C. Klein-Bösing[49] , A. Kluge[34] , M.L. Knichel[91] , A.G. Knospe[111] , C. Kobdaj[34,108] , M. Kofarago[34] , M.K. Köhler[91] , T. Kollegger[39] , A. Kolojvari[123] , V. Kondratiev[123] , N. Kondratyeva[70] , A. Konevskikh[51] , V. Kovalenko[123] , M. Kowalski[110] , S. Kox[65] , G. Koyithatta Meethaleveedu[44] , J. Kral[116] , I. Králik[54] , F. Kramer[48] , A. Kravčáková[38] , M. Krelina[37] , M. Kretz[39] , M. Krivda[96,54] , F. Krizek[77] , E. Kryshen[34] , M. Krzewicki[91] , V. Kučera[77] , Y. Kucheriaev[94,i] , T. Kugathasan[34] , C. Kuhn[50] , P.G. Kuijer[75] , I. Kulakov[48] , J. Kumar[44] , P. Kurashvili[71] , A. Kurepin[51] , A.B. Kurepin[51] , A. Kuryakin[93] , S. Kushpil[77] , M.J. Kweon[87] , Y. Kwon[130] , P. Ladron de Guevara[58] , C. Lagana Fernandes[113] , I. Lakomov[46] , R. Langoy[125] , C. Lara[47] , A. Lardeux[107] , A. Lattuca[25] , S.L. La Pointe[52] , P. La Rocca[27] , R. Lea[24] , G.R. Lee[96] , I. Legrand[34] , J. Lehnert[48] , R.C. Lemmon[76] , V. Lenti[98] , E. Leogrande[52] , M. Leoncino[25] , I. León Monzón[112] , P. Lévai[128] , S. Li[7,64] , J. Lien[125] , R. Lietava[96] , S. Lindal[21] , V. Lindenstruth[39] , C. Lippmann[91] , M.A. Lisa[19] , H.M. Ljunggren[32] , D.F. Lodato[52] , P.I. Loenne[17] , V.R. Loggins[127] , V. Loginov[70] , D. Lohner[87] , C. Loizides[68] , X. Lopez[64] , E. López Torres[9] , X.-G. Lu[87] , P. Luettig[48] , M. Lunardon[28] , G. Luparello[52] , R. Ma[129] , A. Maevskaya[51] , M. Mager[34] , D.P. Mahapatra[56] , S.M. Mahmood[21] , A. Maire[87] , R.D. Majka[129] , M. Malaev[79] , I. Maldonado Cervantes[58] , L. Malinina[iv,61] , D. Mal'Kevich[53] , P. Malzacher[91] , A. Mamonov[93] , L. Manceau[105] , V. Manko[94] , F. Manso[64] , V. Manzari[98] , M. Marchisone[64,25] , J. Mareš[55] , G.V. Margagliotti[24] , A. Margotti[99] , A. Marín[91] , C. Markert[111] , M. Marquard[48] , I. Martashvili[118] , N.A. Martin[91] , P. Martinengo[34] , M.I. Martínez[2] , G. Martínez García[107] , J. Martin Blanco[107] , Y. Martynov[3] , A. Mas[107] , S. Masciocchi[91] , M. Masera[25] , A. Masoni[100] , L. Massacrier[107] , A. Mastroserio[31] , A. Matyja[110] , C. Mayer[110] , J. Mazer[118] , M.A. Mazzoni[103] , F. Meddi[22] , A. Menchaca-Rocha[59] , J. Mercado Pérez[87] , M. Meres[36] , Y. Miake[120] , K. Mikhaylov[61,53] , L. Milano[34] , J. Milosevic[v,21] , A. Mischke[52] , A.N. Mishra[45] , D. Miśkowiec[91] , J. Mitra[124] , C.M. Mitu[57] , J. Mlynarz[127] , N. Mohammadi[52] , B. Mohanty[73,124] , L. Molnar[50] , L. Montaño Zetina[11] , E. Montes[10] , M. Morando[28] , D.A. Moreira De Godoy[113] , S. Moretto[28] , A. Morsch[34] , V. Muccifora[66] , E. Mudnic[109] , D. Mühlheim[49] , S. Muhuri[124] , M. Mukherjee[124] , H. Müller[34] , M.G. Munhoz[113] , S. Murray[83] , L. Musa[34] , J. Musinsky[54] , B.K. Nandi[44] , R. Nania[99] , E. Nappi[98] , C. Nattrass[118] , K. Nayak[73] , T.K. Nayak[124] , S. Nazarenko[93] , A. Nedosekin[53] , M. Nicassio[91] , M. Niculescu[34,57] , B.S. Nielsen[74] , S. Nikolaev[94] , S. Nikulin[94] , V. Nikulin[79] , B.S. Nilsen[80] , F. Noferini[12,99] , P. Nomokonov[61] , G. Nooren[52] , J. Norman[117] , A. Nyanin[94] , J. Nystrand[17] , H. Oeschler[87] , S. Oh[129] , S.K. Oh[vi,40] , A. Okatan[63] , L. Olah[128] , J. Oleniacz[126] , A.C. Oliveira Da Silva[113] , J. Onderwaater[91] , C. Oppedisano[105] , A. Ortiz Velasquez[32] , A. Oskarsson[32] , J. Otwinowski[91] , K. Oyama[87] , P. Sahoo[45] , Y. Pachmayer[87] , M. Pachr[37] , P. Pagano[29] , G. Paić[58] , F. Painke[39] , C. Pajares[16] , S.K. Pal[124] , A. Palmeri[101] , D. Pant[44] , V. Papikyan[1] , G.S. Pappalardo[101] , P. Pareek[45] , W.J. Park[91] , S. Parmar[81] , A. Passfeld[49] , D.I. Patalakha[106] , V. Paticchio[98] , B. Paul[95] , T. Pawlak[126] , T. Peitzmann[52] , H. Pereira Da Costa[14] , E. Pereira De Oliveira Filho[113] , D. Peresunko[94] , C.E. Pérez Lara[75] , A. Pesci[99] , V. Peskov[48] , Y. Pestov[5] , V. Petráček[37] , M. Petran[37] , M. Petris[72] , M. Petrovici[72] , C. Petta[27] , S. Piano[104] , M. Pikna[36] , P. Pillot[107] , O. Pinazza[99,34] , L. Pinsky[115] , D.B. Piyarathna[115] , M. Płoskoń[68] , M. Planinic[121,92] , J. Pluta[126] , S. Pochybova[128] , P.L.M. Podesta-Lerma[112] , M.G. Poghosyan[34] , E.H.O. Pohjoisaho[42] , B. Polichtchouk[106] , N. Poljak[92] , A. Pop[72] , S. Porteboeuf-Houssais[64] , J. Porter[68] , B. Potukuchi[84] , S.K. Prasad[127] , R. Preghenella[99,12] , F. Prino[105] , C.A. Pruneau[127] , I. Pshenichnov[51] , G. Puddu[23] , P. Pujahari[127] , V. Punin[93] , J. Putschke[127] , H. Qvigstad[21] , A. Rachevski[104] , S. Raha[4] , J. Rak[116] , A. Rakotozafindrabe[14] , L. Ramello[30] , R. Raniwala[85] , S. Raniwala[85] , S.S. Räsänen[42] , B.T. Rascanu[48] , D. Rathee[81] , A.W. Rauf[15] , V. Razazi[23] , K.F. Read[118] , J.S. Real[65] , K. Redlich[vii,71] , R.J. Reed[129] , A. Rehman[17] , P. Reichelt[48] , M. Reicher[52] , F. Reidt[34] , R. Renfordt[48] , A.R. Reolon[66] , A. Reshetin[51] , F. Rettig[39] , J.-P. Revol[34] , K. Reygers[87] , V. Riabov[79] , R.A. Ricci[67] , T. Richert[32] , M. Richter[21] , P. Riedler[34] , W. Riegler[34] , F. Riggi[27] , A. Rivetti[105] , E. Rocco[52] , M. Rodríguez Cahuantzi[2] , A. Rodriguez Manso[75] , K. Røed[21] , E. Rogochaya[61] , S. Rohni[84] , D. Rohr[39] , D. Röhrich[17] , R. Romita[76] , F. Ronchetti[66] , L. Ronflette[107] , P. Rosnet[64] , A. Rossi[34] , F. Roukoutakis[82] , A. Roy[45] , C. Roy[50] , P. Roy[95] , A.J. Rubio Montero[10] , R. Rui[24] , R. Russo[25] , E. Ryabinkin[94] , Y. Ryabov[79] , A. Rybicki[110] , S. Sadovsky[106] , K. Šafařík[34] , B. Sahlmuller[48] , R. Sahoo[45] , P.K. Sahu[56] , J. Saini[124] , S. Sakai[68] , C.A. Salgado[16] , J. Salzwedel[19] , S. Sambyal[84] , V. Samsonov[79] , X. Sanchez Castro[50] , F.J. Sánchez Rodríguez[112] , L. Šándor[54] , A. Sandoval[59] , M. Sano[120] , G. Santagati[27] , D. Sarkar[124] , E. Scapparone[99] , F. Scarlassara[28] , R.P. Scharenberg[89] , C. Schiaua[72] , R. Schicker[87] , C. Schmidt[91] , H.R. Schmidt[33] , S. Schuchmann[48] , J. Schukraft[34] , M. Schulc[37] , T. Schuster[129] ,

Y. Schutz[107,34], K. Schwarz[91], K. Schweda[91], G. Scioli[26], E. Scomparin[105], R. Scott[118], G. Segato[28], J.E. Seger[80], Y. Sekiguchi[119], I. Selyuzhenkov[91], J. Seo[90], E. Serradilla[10,59], A. Sevcenco[57], A. Shabetai[107], G. Shabratova[61], R. Shahoyan[34], A. Shangaraev[106], N. Sharma[118], S. Sharma[84], K. Shigaki[43], K. Shtejer[25], Y. Sibiriak[94], S. Siddhanta[100], T. Siemiarczuk[71], D. Silvermyr[78], C. Silvestre[65], G. Simatovic[121], R. Singaraju[124], R. Singh[84], S. Singha[124,73], V. Singhal[124], B.C. Sinha[124], T. Sinha[95], B. Sitar[36], M. Sitta[30], T.B. Skaali[21], K. Skjerdal[17], M. Slupecki[116], N. Smirnov[129], R.J.M. Snellings[52], C. Søgaard[32], R. Soltz[69], J. Song[90], M. Song[130], F. Soramel[28], S. Sorensen[118], M. Spacek[37], E. Spiriti[66], I. Sputowska[110], M. Spyropoulou-Stassinaki[82], B.K. Srivastava[89], J. Stachel[87], I. Stan[57], G. Stefanek[71], M. Steinpreis[19], E. Stenlund[32], G. Steyn[60], J.H. Stiller[87], D. Stocco[107], M. Stolpovskiy[106], P. Strmen[36], A.A.P. Suaide[113], T. Sugitate[43], C. Suire[46], M. Suleymanov[15], R. Sultanov[53], M. Šumbera[77], T. Susa[92], T.J.M. Symons[68], A. Szabo[36], A. Szanto de Toledo[113], I. Szarka[36], A. Szczepankiewicz[34], M. Szymanski[126], J. Takahashi[114], M.A. Tangaro[31], J.D. Tapia Takaki[i,viii,46], A. Tarantola Peloni[48], A. Tarazona Martinez[34], M.G. Tarzila[72], A. Tauro[34], G. Tejeda Muñoz[2], A. Telesca[34], C. Terrevoli[23], J. Thäder[91], D. Thomas[52], R. Tieulent[122], A.R. Timmins[115], A. Toia[102], V. Trubnikov[3], W.H. Trzaska[116], T. Tsuji[119], A. Tumkin[93], R. Turrisi[102], T.S. Tveter[21], K. Ullaland[17], A. Uras[122], G.L. Usai[23], M. Vajzer[77], M. Vala[54,61], L. Valencia Palomo[64], S. Vallero[87], P. Vande Vyvre[34], J. Van Der Maarel[52], J.W. Van Hoorne[34], M. van Leeuwen[52], A. Vargas[2], M. Vargyas[116], R. Varma[44], M. Vasileiou[82], A. Vasiliev[94], V. Vechernin[123], M. Veldhoen[52], A. Velure[17], M. Venaruzzo[24,67], E. Vercellin[25], S. Vergara Limón[2], R. Vernet[8], M. Verweij[127], L. Vickovic[109], G. Viesti[28], J. Viinikainen[116], Z. Vilakazi[60], O. Villalobos Baillie[96], A. Vinogradov[94], L. Vinogradov[123], Y. Vinogradov[93], T. Virgili[29], Y.P. Viyogi[124], A. Vodopyanov[61], M.A. Völkl[87], K. Voloshin[53], S.A. Voloshin[127], G. Volpe[34], B. von Haller[34], I. Vorobyev[123], D. Vranic[91,34], J. Vrláková[38], B. Vulpescu[64], A. Vyushin[93], B. Wagner[17], J. Wagner[91], V. Wagner[37], M. Wang[7,107], Y. Wang[87], D. Watanabe[120], M. Weber[115], J.P. Wessels[49], U. Westerhoff[49], J. Wiechula[33], J. Wikne[21], M. Wilde[49], G. Wilk[71], J. Wilkinson[87], M.C.S. Williams[99], B. Windelband[87], M. Winn[87], C.G. Yaldo[127], Y. Yamaguchi[119], H. Yang[52], P. Yang[7], S. Yang[17], S. Yano[43], S. Yasnopolskiy[94], J. Yi[90], Z. Yin[7], I.-K. Yoo[90], I. Yushmanov[94], V. Zaccolo[74], C. Zach[37], A. Zaman[15], C. Zampolli[99], S. Zaporozhets[61], A. Zarochentsev[123], P. Závada[55], N. Zaviyalov[93], H. Zbroszczyk[126], I.S. Zgura[57], M. Zhalov[79], H. Zhang[7], X. Zhang[7,68], Y. Zhang[7], C. Zhao[21], N. Zhigareva[53], D. Zhou[7], F. Zhou[7], Y. Zhou[52], Zhou, Zhuo[17], H. Zhu[7], J. Zhu[7], X. Zhu[7], A. Zichichi[12,26], A. Zimmermann[87], M.B. Zimmermann[49,34], G. Zinovjev[3], Y. Zoccarato[122], M. Zyzak[48]

Affiliation notes

[i] Deceased
[ii] Also at: St. Petersburg State Polytechnical University
[iii] Also at: Department of Applied Physics, Aligarh Muslim University, Aligarh, India
[iv] Also at: M.V. Lomonosov Moscow State University, D.V. Skobeltsyn Institute of Nuclear Physics, Moscow, Russia
[v] Also at: University of Belgrade, Faculty of Physics and "Vinča" Institute of Nuclear Sciences, Belgrade, Serbia
[vi] Permanent Address: Permanent Address: Konkuk University, Seoul, Korea
[vii] Also at: Institute of Theoretical Physics, University of Wroclaw, Wroclaw, Poland
[viii] Also at: University of Kansas, Lawrence, KS, United States

Collaboration Institutes

[1] A.I. Alikhanyan National Science Laboratory (Yerevan Physics Institute) Foundation, Yerevan, Armenia
[2] Benemérita Universidad Autónoma de Puebla, Puebla, Mexico
[3] Bogolyubov Institute for Theoretical Physics, Kiev, Ukraine
[4] Bose Institute, Department of Physics and Centre for Astroparticle Physics and Space Science (CAPSS), Kolkata, India
[5] Budker Institute for Nuclear Physics, Novosibirsk, Russia
[6] California Polytechnic State University, San Luis Obispo, CA, United States
[7] Central China Normal University, Wuhan, China
[8] Centre de Calcul de l'IN2P3, Villeurbanne, France
[9] Centro de Aplicaciones Tecnológicas y Desarrollo Nuclear (CEADEN), Havana, Cuba
[10] Centro de Investigaciones Energéticas Medioambientales y Tecnológicas (CIEMAT), Madrid, Spain
[11] Centro de Investigación y de Estudios Avanzados (CINVESTAV), Mexico City and Mérida, Mexico

[12] Centro Fermi - Museo Storico della Fisica e Centro Studi e Ricerche "Enrico Fermi", Rome, Italy
[13] Chicago State University, Chicago, USA
[14] Commissariat à l'Energie Atomique, IRFU, Saclay, France
[15] COMSATS Institute of Information Technology (CIIT), Islamabad, Pakistan
[16] Departamento de Física de Partículas and IGFAE, Universidad de Santiago de Compostela, Santiago de Compostela, Spain
[17] Department of Physics and Technology, University of Bergen, Bergen, Norway
[18] Department of Physics, Aligarh Muslim University, Aligarh, India
[19] Department of Physics, Ohio State University, Columbus, OH, United States
[20] Department of Physics, Sejong University, Seoul, South Korea
[21] Department of Physics, University of Oslo, Oslo, Norway
[22] Dipartimento di Fisica dell'Università 'La Sapienza' and Sezione INFN Rome, Italy
[23] Dipartimento di Fisica dell'Università and Sezione INFN, Cagliari, Italy
[24] Dipartimento di Fisica dell'Università and Sezione INFN, Trieste, Italy
[25] Dipartimento di Fisica dell'Università and Sezione INFN, Turin, Italy
[26] Dipartimento di Fisica e Astronomia dell'Università and Sezione INFN, Bologna, Italy
[27] Dipartimento di Fisica e Astronomia dell'Università and Sezione INFN, Catania, Italy
[28] Dipartimento di Fisica e Astronomia dell'Università and Sezione INFN, Padova, Italy
[29] Dipartimento di Fisica 'E.R. Caianiello' dell'Università and Gruppo Collegato INFN, Salerno, Italy
[30] Dipartimento di Scienze e Innovazione Tecnologica dell'Università del Piemonte Orientale and Gruppo Collegato INFN, Alessandria, Italy
[31] Dipartimento Interateneo di Fisica 'M. Merlin' and Sezione INFN, Bari, Italy
[32] Division of Experimental High Energy Physics, University of Lund, Lund, Sweden
[33] Eberhard Karls Universität Tübingen, Tübingen, Germany
[34] European Organization for Nuclear Research (CERN), Geneva, Switzerland
[35] Faculty of Engineering, Bergen University College, Bergen, Norway
[36] Faculty of Mathematics, Physics and Informatics, Comenius University, Bratislava, Slovakia
[37] Faculty of Nuclear Sciences and Physical Engineering, Czech Technical University in Prague, Prague, Czech Republic
[38] Faculty of Science, P.J. Šafárik University, Košice, Slovakia
[39] Frankfurt Institute for Advanced Studies, Johann Wolfgang Goethe-Universität Frankfurt, Frankfurt, Germany
[40] Gangneung-Wonju National University, Gangneung, South Korea
[41] Gauhati University, Department of Physics, Guwahati, India
[42] Helsinki Institute of Physics (HIP), Helsinki, Finland
[43] Hiroshima University, Hiroshima, Japan
[44] Indian Institute of Technology Bombay (IIT), Mumbai, India
[45] Indian Institute of Technology Indore, Indore (IITI), India
[46] Institut de Physique Nucléaire d'Orsay (IPNO), Université Paris-Sud, CNRS-IN2P3, Orsay, France
[47] Institut für Informatik, Johann Wolfgang Goethe-Universität Frankfurt, Frankfurt, Germany
[48] Institut für Kernphysik, Johann Wolfgang Goethe-Universität Frankfurt, Frankfurt, Germany
[49] Institut für Kernphysik, Westfälische Wilhelms-Universität Münster, Münster, Germany
[50] Institut Pluridisciplinaire Hubert Curien (IPHC), Université de Strasbourg, CNRS-IN2P3, Strasbourg, France
[51] Institute for Nuclear Research, Academy of Sciences, Moscow, Russia
[52] Institute for Subatomic Physics of Utrecht University, Utrecht, Netherlands
[53] Institute for Theoretical and Experimental Physics, Moscow, Russia
[54] Institute of Experimental Physics, Slovak Academy of Sciences, Košice, Slovakia
[55] Institute of Physics, Academy of Sciences of the Czech Republic, Prague, Czech Republic
[56] Institute of Physics, Bhubaneswar, India
[57] Institute of Space Science (ISS), Bucharest, Romania
[58] Instituto de Ciencias Nucleares, Universidad Nacional Autónoma de México, Mexico City, Mexico
[59] Instituto de Física, Universidad Nacional Autónoma de México, Mexico City, Mexico
[60] iThemba LABS, National Research Foundation, Somerset West, South Africa
[61] Joint Institute for Nuclear Research (JINR), Dubna, Russia
[62] Korea Institute of Science and Technology Information, Daejeon, South Korea

[63] KTO Karatay University, Konya, Turkey
[64] Laboratoire de Physique Corpusculaire (LPC), Clermont Université, Université Blaise Pascal, CNRS–IN2P3, Clermont-Ferrand, France
[65] Laboratoire de Physique Subatomique et de Cosmologie, Université Grenoble-Alpes, CNRS-IN2P3, Grenoble, France
[66] Laboratori Nazionali di Frascati, INFN, Frascati, Italy
[67] Laboratori Nazionali di Legnaro, INFN, Legnaro, Italy
[68] Lawrence Berkeley National Laboratory, Berkeley, CA, United States
[69] Lawrence Livermore National Laboratory, Livermore, CA, United States
[70] Moscow Engineering Physics Institute, Moscow, Russia
[71] National Centre for Nuclear Studies, Warsaw, Poland
[72] National Institute for Physics and Nuclear Engineering, Bucharest, Romania
[73] National Institute of Science Education and Research, Bhubaneswar, India
[74] Niels Bohr Institute, University of Copenhagen, Copenhagen, Denmark
[75] Nikhef, National Institute for Subatomic Physics, Amsterdam, Netherlands
[76] Nuclear Physics Group, STFC Daresbury Laboratory, Daresbury, United Kingdom
[77] Nuclear Physics Institute, Academy of Sciences of the Czech Republic, Řež u Prahy, Czech Republic
[78] Oak Ridge National Laboratory, Oak Ridge, TN, United States
[79] Petersburg Nuclear Physics Institute, Gatchina, Russia
[80] Physics Department, Creighton University, Omaha, NE, United States
[81] Physics Department, Panjab University, Chandigarh, India
[82] Physics Department, University of Athens, Athens, Greece
[83] Physics Department, University of Cape Town, Cape Town, South Africa
[84] Physics Department, University of Jammu, Jammu, India
[85] Physics Department, University of Rajasthan, Jaipur, India
[86] Physik Department, Technische Universität München, Munich, Germany
[87] Physikalisches Institut, Ruprecht-Karls-Universität Heidelberg, Heidelberg, Germany
[88] Politecnico di Torino, Turin, Italy
[89] Purdue University, West Lafayette, IN, United States
[90] Pusan National University, Pusan, South Korea
[91] Research Division and ExtreMe Matter Institute EMMI, GSI Helmholtzzentrum für Schwerionenforschung, Darmstadt, Germany
[92] Rudjer Bošković Institute, Zagreb, Croatia
[93] Russian Federal Nuclear Center (VNIIEF), Sarov, Russia
[94] Russian Research Centre Kurchatov Institute, Moscow, Russia
[95] Saha Institute of Nuclear Physics, Kolkata, India
[96] School of Physics and Astronomy, University of Birmingham, Birmingham, United Kingdom
[97] Sección Física, Departamento de Ciencias, Pontificia Universidad Católica del Perú, Lima, Peru
[98] Sezione INFN, Bari, Italy
[99] Sezione INFN, Bologna, Italy
[100] Sezione INFN, Cagliari, Italy
[101] Sezione INFN, Catania, Italy
[102] Sezione INFN, Padova, Italy
[103] Sezione INFN, Rome, Italy
[104] Sezione INFN, Trieste, Italy
[105] Sezione INFN, Turin, Italy
[106] SSC IHEP of NRC Kurchatov institute, Protvino, Russia
[107] SUBATECH, Ecole des Mines de Nantes, Université de Nantes, CNRS-IN2P3, Nantes, France
[108] Suranaree University of Technology, Nakhon Ratchasima, Thailand
[109] Technical University of Split FESB, Split, Croatia
[110] The Henryk Niewodniczanski Institute of Nuclear Physics, Polish Academy of Sciences, Cracow, Poland
[111] The University of Texas at Austin, Physics Department, Austin, TX, USA
[112] Universidad Autónoma de Sinaloa, Culiacán, Mexico
[113] Universidade de São Paulo (USP), São Paulo, Brazil
[114] Universidade Estadual de Campinas (UNICAMP), Campinas, Brazil
[115] University of Houston, Houston, TX, United States

[116] University of Jyväskylä, Jyväskylä, Finland
[117] University of Liverpool, Liverpool, United Kingdom
[118] University of Tennessee, Knoxville, TN, United States
[119] University of Tokyo, Tokyo, Japan
[120] University of Tsukuba, Tsukuba, Japan
[121] University of Zagreb, Zagreb, Croatia
[122] Université de Lyon, Université Lyon 1, CNRS/IN2P3, IPN-Lyon, Villeurbanne, France
[123] V. Fock Institute for Physics, St. Petersburg State University, St. Petersburg, Russia
[124] Variable Energy Cyclotron Centre, Kolkata, India
[125] Vestfold University College, Tonsberg, Norway
[126] Warsaw University of Technology, Warsaw, Poland
[127] Wayne State University, Detroit, MI, United States
[128] Wigner Research Centre for Physics, Hungarian Academy of Sciences, Budapest, Hungary
[129] Yale University, New Haven, CT, United States
[130] Yonsei University, Seoul, South Korea
[131] Zentrum für Technologietransfer und Telekommunikation (ZTT), Fachhochschule Worms, Worms, Germany